

# TESTING COUPLED MCNP6/CTF ON AN ASSEMBLY LEVEL PROBLEM WITH AN ACCELERATION TECHNIQUE

A. Bennett, K. Ivanov, M. Avramova

Department of Mechanical and Nuclear Engineering  
137 Reber Building, University Park, PA 16802  
asb241@psu.edu; kni1@psu.edu; mna109@psu.edu

## Abstract

There has been a recent trend towards Monte Carlo based multi-physics codes to obtain high accuracy reactor core solutions. These high accuracy solutions can be used as reference solutions to validate deterministic codes. To obtain this high accuracy solution, a high fidelity coupled code was created. The coupling is done between a Monte Carlo code and a Thermal Hydraulic code. The use of a Monte Carlo code allows exact geometry modeling, as well as the use of continuous energy cross sections. Coupling with a Thermal Hydraulic code will allow the feedback effects to be accurately modeled. The coupling is done between MCNP6, which is a general purpose Monte Carlo transport code, and CTF, which is a sub-channel code. The coupling was performed using an internal coupling method for each pin and axial level.

Most of the research done on these coupled codes is done initially on small systems, such as single pins or mini assemblies in order to verify the functionality of the coupling scheme. In this paper, the coupled MCNP6/CTF is tested on a full assembly level problem. The main drawbacks of using a Monte Carlo code in the coupled system are the high computational requirement and the statistical noise that is added to the solution. A relaxation acceleration technique is applied to the coupled code. The acceleration technique showed similar results when using the same convergence criteria and showed decreasing the statistical error on the solution with increasing number of iterations. This also allows a stricter coupled convergence criterion to be utilized as compared to the standard coupling approach.

## KEYWORDS

Coupled, MCNP6, CTF, Acceleration, Assembly

## 1. Introduction

There has been a recent trend towards Monte Carlo based multi-physics codes to get more accurate reactor core solutions. There are many different types of multi-physics couplings. This paper will be focusing on a coupled Monte Carlo and thermal-hydraulics subchannel code. Monte Carlo codes can take advantage of exact geometry modeling and continuous energy cross sections. Coupling with a thermal-hydraulics subchannel code allows for accurate modeling of the feedback effects in an efficient manner.

The trend towards Monte Carlo based multi-physics codes has been driven by the need for more reference solutions at operating conditions for deterministic codes. For each new reactor design, deterministic codes need reference solutions to make sure they are accurately modeling the reactor. Creating reference solutions through experiments has become costly and difficult. Instead, high fidelity multi-physics codes have been calculating reference solutions to validate the deterministic codes. To achieve this high fidelity

solution, the internal coupling between a Monte Carlo code and a subchannel code is done at each pin and axial level.

There are currently many different coupled Monte Carlo/thermal-hydraulic codes. Some of these codes use older and possibly outdated codes. The coupling scheme described in this paper uses MCNP6 and CTF. CTF is the modernized version of COBRA-TF, maintained and developed at Pennsylvania State University (PSU). This is the version being utilized also in the Consortium for Advanced Simulation of Light Water Reactors (LWRs) - CASL - activities.

Most of these coupled codes have only been tested on small systems, such as a single pin or a mini assembly. This is due to the high computation costs of these coupled code systems. The coupled Monte Carlo/thermal-hydraulics code described in this paper is run on a full three dimensional (3D) assembly level test problem. The main drawbacks of using a Monte Carlo code in the coupled system are the high computational requirements and the statistical noise that is added into the solution. A relaxation acceleration technique is applied to the coupled code to reduce these drawbacks.

The previous work that has been done on this coupled code involved smaller geometries, including either a single pin or a pin array. These results were compared with other coupled Monte Carlo/thermal-hydraulic codes and gave similar results. These results can be found in [1]. The objective of this paper is to show that the coupled code can be applied to larger test problems, such as a full 3D assembly model with cross-flows modeled by the subchannel code and to demonstrate the benefit of using a relaxation acceleration technique in coupled Monte Carlo/ thermal hydraulic calculations.

## **2. Codes**

Within the coupled code, the Monte Carlo code is MCNP6 and the thermal hydraulic code is CTF. Additionally, the codes `fit_otf` and `makxsf` are also used in cross section generation. These additional codes are included with MCNP6.

### **2.1. MCNP6**

MCNP stands for Monte Carlo N-Particle [2]. MCNP6 is a three-dimensional general purpose Monte Carlo transport code that solves the integral transport equation. MCNP6 has exact geometry modeling, uses continuous energy cross sections, incorporates features supporting thermal-hydraulic feedback, and includes options for burnup/depletion calculations. This code was chosen for the coupling since it is well maintained and documented, previous work at Penn State has been done on a coupled MCNP5/CTF, and includes options for On-The-Fly cross sections and burnup capabilities.

For the purpose of the coupled code, MCNP6 will be running criticality calculations. It will calculate relative power profiles and the k-eff of the system. MCNP6 uses continuous energy cross sections. To create these cross sections at the correct temperatures, the codes `fit_otf` and `makxsf` are used.

#### **1.1.1. `fit_otf`**

`fit_otf` creates the On-The-Fly cross sections that can be used by MCNP6 [3]. The On-The-Fly cross sections describe the cross section as a function of both energy and temperature. This is done by creating up to a 17 term functional expansion of the cross section in temperature. These cross sections can be created over the temperature range of 250K to 3200K. It has been shown that these On-The-Fly cross sections can be generated to have a fraction tolerance of 0.1% to the actual cross section in [3]. This code allows for only one cross section file to be created for each isotope rather than having to create a cross section file for each temperature and each isotope.

### 1.1.2. makxf

The `fit_otf` code does not create On-The-Fly cross sections for thermal scattering. To add this element, the `makxf` code was used [4]. This is a program that manipulates cross section libraries for MCNP. Some of the capabilities of the `makxf` code include: Doppler broadening of resolved cross section data, and interpolating thermal scattering kernels and unresolved resonance cross section data between two temperatures. For the purpose of the coupled code, `makxf` is used to create new thermal scattering libraries at various temperatures and interpolates in them.

## 1.2. CTF

CTF is the improved PSU and CASL version of COBRA-TF, which stands for Coolant Boiling in Rod Arrays – Two Fluid [5]. Cobra-TF is a 3D thermal-hydraulic simulation code designed for Light Water Reactor (LWR) vessel and core analysis. It uses a two-fluid, three-field modeling approach. CTF is a thermal-hydraulic subchannel code that solves three momentum conservation equations, four mass conservation equations and two energy conservation equations. Since CTF is a two-phase code, it has the ability to model both PWR and BWR conditions. CTF's modeling advantages include a three-field representation of vapor, continuous liquid, and liquid droplets, and the ability to model fully three-dimensional heat conduction, and dynamic gap conduction between the fuel pellet and cladding. Improvements at PSU and within CASL have included development of models, enhancing computational efficiency, extensive verification, validation, and uncertainty quantification as well as improving software quality and documentation of CTF. In the radial plane for pin-by-pin conditions CTF can utilize either subchannel-centered model of the coolant flow between pins or rod-centered model. These two models lead to different spatial coupling schemes with neutronic codes. In this paper for spatial coupling with MCNP6, the rod-centered model of CTF is used.

Within the coupled code, CTF calculates all the thermal hydraulic feedback parameters. The thermal hydraulic feedback parameters include the temperature of the fuel, cladding, and moderator as well as the density of the moderator.

## 3. Coupling Scheme

When coupling codes together, it is important that the geometry must be consistently mapped between the codes. This allows for accurate pre-passing of the thermal hydraulic feedback effects and the power profiles. These feedback values have to be updated before each iteration of the coupled code. After running a sufficient number of iterations of the coupled code, a converged solution can be obtained.

### 3.1. Geometry Mapping

Optimum geometry mapping occurs when the exact same geometry is modeled in both codes. Synchronous geometry mapping is accomplished within the coupled MCNP6/CTF code described in this paper. MCNP6 has a generalized geometry to be able to model the exact geometry. In the case of the coupled code, this allows MCNP6 to model the CTF geometry exactly. After the same geometry is modeled in both codes, the geometry can be mapped between the two codes. The mapping is achieved by adding three additional cell cards options in MCNP6. The first cell card option is to specify what type of material is located in the cell (fuel, cladding, or moderator), the second cell card option specifies the location of the cell (fuel pin number or sub-channel number in reference to CTF's numbering) and the last cell card option specifies the axial location (in reference to CTF's numbering) of the cell. In addition to

the cell card options, the thermal scattering numbering and the tallying numbering must be given in a specific format to perform the rest of the geometry mapping. The downside of this geometry mapping, is the length of the input file required by MCNP6 in the coupled code. A cell card has to be created for each axial and radial cell in CTF for the fuel, cladding and moderator. In addition, a new material card has to be created for each axial and radial cell in the moderator and F4 neutron tallies have to be created for each fuel cell card.

### 3.2. Temperature Dependence

The feedback temperatures calculated by CTF are volume-averaged temperatures. In the fuel pin, there can be a large difference in temperature from the centerline to outside of the pin. This requires many radial fuel regions per pin to be modeled to get an accurate fuel temperature. In the test problems given in the paper, the number of fuel regions was set to 10 radial regions.

To accurately account for the temperature dependence within MCNP6, both the cross sections and the thermal scattering cross sections have to be broadened to the correct temperature. Previously, this was done by creating new cross sections files at various temperatures. This can be done in one of two ways, either by creating a new cross section file at every temperature needed by the simulation or by creating a new cross section file at temperature increments and then mixing these cross sections to get the correct temperature dependence. In both of these methods, many large cross-section files are needed.

With the addition of fit\_otf into MCNP6, it is much easier to handle the temperature dependence of the cross sections. fit\_otf creates a functional expansion of the cross section in temperature. It has been shown that using a 17 term expansion, with an energy grid of 50K and a temperature grid of 10K, the On-The-Fly cross sections can have a fractional tolerance of 0.1% to the actual cross sections [3]. For the test problems given in this paper, the energy grid was refined to 10K and the temperature grid was refined to 2K. Using these On-The-Fly cross sections allows only one cross section file to be created for each isotope rather than a cross section file for each isotope and each energy grid point.

The thermal scattering cross sections cannot be created using fit\_otf. Instead new thermal scattering cross sections files are created for every 1K over the temperature range of the moderator. These cross section files are created using makssf.

### 3.3. Coupled Calculation

The flow chart of the coupled code is shown in Fig. 1. The calculation is started with CTF. The user must specify the initial power profile. The closer the initial power profile is to the converged power profile, the lower amount of total iterations is required. If this is not the first iteration, the power profiles that are used in CTF are obtained from the previous MCNP6 calculation. After the CTF calculation has been performed, the thermal hydraulic feedback parameters are calculated. The thermal hydraulic feedback parameters include the temperatures of the fuel, cladding and moderator as well as the density of the moderator. Coupled code convergence is then checked in Eq. 1.

$$\varepsilon \geq \max_{i,j} \left| \frac{T_{i,j}^{current} - T_{i,j}^{previous}}{T_{i,j}^{previous}} \right| \quad (1)$$

Where  $\varepsilon$  is the convergence criteria,  $T$  is the temperature in Kelvin,  $i$  is the rod number and  $j$  is the axial node number. If Eq. 1 is true for all the rods and axial levels then convergence has been met and the total calculation is over, but if it is false, then MCNP6 is run with the new feedback parameters calculated by CTF. MCNP6 calculates new power profiles and they are passed back to CTF, to start a new coupled

iteration.

Convergence is checked for the temperature of the fuel and the temperature of the moderator in Kelvin for all rods, sub-channels and axial levels. It is not applied to the power profiles due to statistical uncertainties. The statistical uncertainties also have a lesser effect on the temperatures but they should be taken into account when choosing convergence criteria.

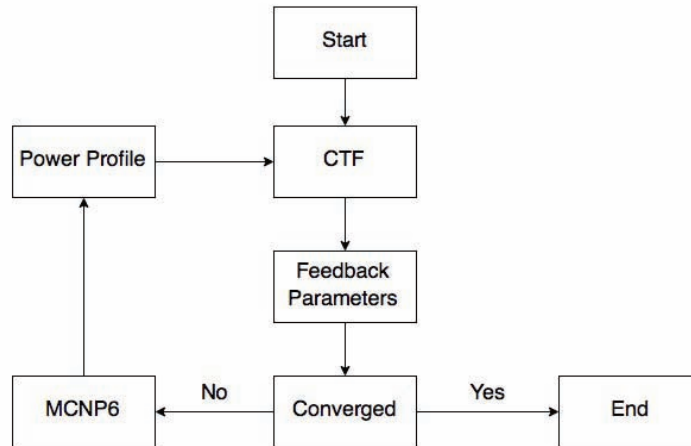


**Figure 1 - Flow Chart of the Coupled Code**

### 3.4. Coupling Method

There are two types of coupling methods, internally and externally coupling. External coupling is usually easier to implement since this method does not require changing the source code for the codes being coupled. The information is just updated through the input files. Internal coupling is commonly faster since it does not require reading and writing between iterations. This method also does not have to initialize the codes for each new coupled code iteration. This results in a significant decrease in time, since MCNP6 can have large initialization times for complex problems. As a result, the internally coupled method was chosen due to the fact that it reduces computational time.

In the coupling scheme, MCNP was chosen as the master program and the CTF source code was added as a subfolder in the MCNP source code. The internal coupling method was implemented by adding new subroutines into the MCNP source code. The main subroutine that was added into the MCNP source was an iterate subroutine. This subroutine would iterate between running MCNP and CTF. The iterate subroutine would also call functions that would calculate the new feedback parameters and power profiles for MCNP and CTF. To update CTF with new power profiles and obtain the resulting feedback parameters was simply achieved by using the coupling interface that has been implemented in the CASL version of CTF. Passing information with MCNP was more challenging since there was not an available coupling interface. To update the feedback information in MCNP, the input variable array (stores temperatures and densities) and the thermal scattering cross sections is updated before each MCNP calculation. The new power profiles were retrieved from MCNP when the tally information was print to the output file. The full double precision of the tally is saved.

#### 4. Relaxation Acceleration

In a coupled Monte Carlo/Thermal-Hydraulic calculation, the steady state flux(or power) is calculated as:

$$\phi = F(T, \rho) \quad (2)$$

where  $T$  is the temperature distribution and  $\rho$  is the density distribution. Both of these distributions depend on the flux from the previous iteration:

$$\phi^n = F(T(\phi^{n-1}), \rho(\phi^{n-1})) \quad (3)$$

where  $n$  is the iteration number. The flux is calculated using Monte Carlo methods. This adds a statistical noise to the answer:

$$R(\phi) = F(T(\phi^{n-1}), \rho(\phi^{n-1})) + \xi \quad (4)$$

Subsequently, the coupled convergence criteria from Eq. 1 will be modified as:

$$\varepsilon \geq \max_{i,j} \left| \frac{T_{i,j}^{current} - T_{i,j}^{previous} + \xi_{i,j}^{current} - \xi_{i,j}^{previous}}{T_{i,j}^{previous} + \xi_{i,j}^{previous}} \right| \quad (5)$$

The convergence of the coupled solution will then be limited to the magnitude of the statistical noise. Keeping this in mind, a technique must be implemented to account for the statistical noise. The flux can be defined as the sum of all the previous fluxes as:

$$\phi^{n+1} = \frac{1}{n} \sum_{i=1}^n R(\phi) \quad (5)$$

Now that since the flux is the mean value of all the previous iterations, the error will decrease with increasing number of iterations. Any convergence criteria can be met if sufficient number of iterations is preformed. Then Eq. 5 can be rearranged:

$$\phi^{n+1} = \left(1 - \frac{1}{n}\right) \frac{1}{n-1} \sum_{i=1}^{n-1} R(\phi^i) + \frac{1}{n} R(\phi^n) = \left(1 - \frac{1}{n}\right) \phi^n + \frac{1}{n} R(\phi^n) \quad (6)$$

This form of the relaxation technique is just a weighted function of the current value of the flux and the previous value of the flux. Eq. 6 gives the explicit formulation of the relaxation scheme. The flux in the next iteration is obtained to be the mean value of all the iterations. Since in essence the tally estimates from all iterations are added together, the error decreases with increasing number of iterations. Moreover, from Eq. 6 follows that the flux from all preceding iterations is reflected in the final solution with a weight of  $1/n$ . In this way the variance is improved with each coupled iteration. Any desired convergence criteria can be satisfied, if a sufficient number of coupled iterations are performed. This is the form of the relaxation technique that was implemented into the coupled code. A more complete derivation of this stochastic approximation can be found in [6].

## 5. Assembly Model

The assembly level problem that was modeled was based on a 17x17 assembly given in [7]. The assembly that was modeled in [7], was their base assembly without any burnable absorber rods. The central instrument tube was modeled as a guide tube. The specifications and geometry for this assembly is given in Fig. 2. The material specification is given in Appendix A. The fuel was modeled as 2.4% enriched  $UO_2$  and the guide tubes were filled with water. The pressure value is a normal operating value for a Pressurized Water Reactor (PWR). No grid spacers were modeled.

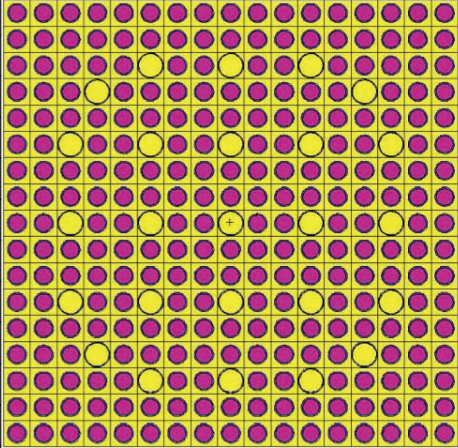
Flow Rate (kg/s)	84.089	
Power (MW)	17.674	
Pressure (MPa)	15.513	
Gap Conductance (W/m <sup>2</sup> K)	6000	
Fuel Density Fraction	0.9387	
Inlet Temperature (C)	293.333	
Fuel Length (cm)	365.76	
Fuel Plenum Length (cm)	30	
Fuel Pitch (cm)	1.25984	
Pellet Radius (cm)	0.39218	
Pin Radius (cm)	0.4572	
Guide Tube Inner Radius (cm)	0.56134	
Guide Tube Outer Radius (cm)	0.60198	

Figure 2 - Assembly Specifications

## 6. Coupled Code Convergence Studies

Using the model given in the previous section, four different test cases were run in order to perform a sensitivity study on coupled code convergence behavior. The four different test cases are:

- 400 Particles/Cycle without Relaxation Acceleration
- 1600 Particles/Cycle without Relaxation Acceleration
- 400 Particles/Cycle with Relaxation Acceleration
- 1600 Particles/Cycle with Relaxation Acceleration

For each case, there were 100 inactive cycles, which converged both the fission source and the eigenvalue. Each case was run for 400 active cycles. Another convergence criterion is the convergence of the fission heat tallies. Ideally you want the tallies to have an error of less than 1%. This can take a significant amount of time for tallies on the outer edge of large problems. Running non-analog Monte Carlo can solve this, but this is left for future work. Instead, 1600 particles/cycle were run to achieve an error of less than 1% on the tallies. Also the case of 400 particles/cycle was also tested which corresponds to an error of less than 2%.

Each test case was run for 9 coupled iterations and the calculated convergence was plotted vs iteration number in Fig. 4. Each line in the plot represents:

- Blue Line: 400 Particles/Cycle without Relaxation Acceleration
- Red Line: 1600 Particles/Cycle without Relaxation Acceleration

- Green Line: 400 Particles/Cycle with Relaxation Acceleration
- Purple Line: 1600 Particles/Cycle with Relaxation Acceleration

After inspecting the plot, the convergence value for comparison of results was chosen to be  $2.5e-2$ , which is shown in Fig. 3 as the light blue line. This convergence value at which results compared was chosen since this was the strictest convergence achieved in the case without Relaxation Acceleration. It can be observed that both cases with relaxation acceleration converged in 3 iterations and the case without the relaxation acceleration converged in 4 iterations. For this particular model and convergence criteria, the relaxation acceleration technique saved one iteration. This will become more pronounced when it is applied to a problem with a more skewed power profile such as for a Boiling Water Reactor (BWR) and to larger computational problems such as mini-cores and core sectors of symmetry. The relaxation acceleration technique was applied to a PWR to show that it still has a positive effect when the power profiles are not skewed and on a single assembly level. Another positive effect of this relaxation acceleration technique is that it is able to achieve stricter coupled convergence criterion than the standard coupling approach can achieve. The convergence obtained from each run is given in Table 1.

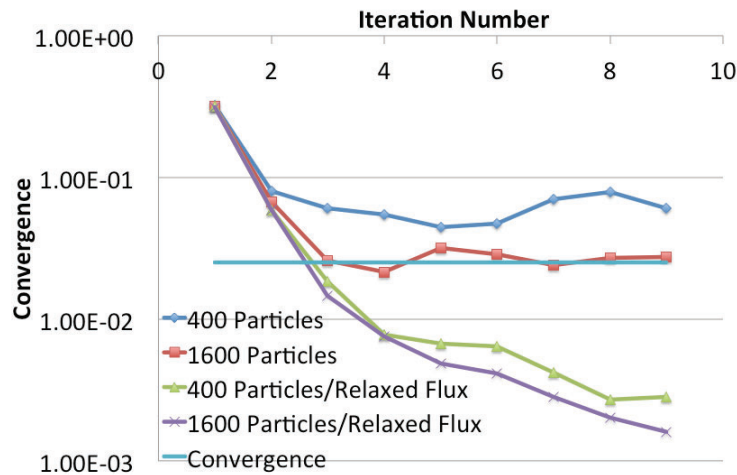


Figure 3 - Convergence vs Coupled Iteration Number

Table 1 - Minimum Convergence Obtained

Test Case	Achieved Convergence
400 Particles	4.46e-2
1600 Particles	2.16e-2
400 Particles/Relaxed Flux	2.69e-3
1600 Particles/Relaxed Flux	1.61e-3



## 7. Relaxation Acceleration Results

The plot of the average axial coolant density distribution over the entire assembly is given in Fig. 4. Each line in the plot represents:

- Blue Line: 1600 Particles/Cycle without Relaxation Acceleration
- Red Line: 400 Particles/Cycle with Relaxation Acceleration
- Green Line: 1600 Particles/Cycle with Relaxation Acceleration

The low-density change over the length of the core is due to the high pressure in a PWR. The density profile shown is expected for a typical PWR.

The plot of the average axial fuel temperature distribution over the entire assembly is given in Fig. 5. The fuel temperature profile has a middle peaked behavior. The plot of the average axial power distribution has a similar shape to the average axial fuel temperature distribution.

As one can see from Fig. 4 and 5, there is not much of a difference in the results between the 3 different coupled runs. To show the difference between the different runs, the average percent difference was calculated for both of the relaxation acceleration runs with reference to the case without the relaxation acceleration. These results are shown in Table 2. As one can see all percent differences are within the coupled code convergence criteria. This shows that relaxation acceleration technique still converges to the correct solution. Another interesting result is that in the case of running 400 particles per cycle, the relaxation acceleration technique was still able to dampen out the larger statistical noise and still converge to the correct solution.

In practicality, the convergence criteria needs to be set much stricter (usually  $\varepsilon = 10^{-4}$ ) when using this acceleration technique. Even though it was shown previously that comparable results were found using the same convergence criteria, the flux is a function of all the previously fluxes so we are just “accelerating” the results towards the convergence criteria. The major advantage of this acceleration technique is not just that one is overcoming the statistical noise that is affecting the coupled convergence but also one can run with less particles. As you can see in the results, similar results were shown between the two cases with the acceleration technique. While one is going to have to run to a much stricter convergence criteria with this technique, running less particles will help to decrease this computational cost.

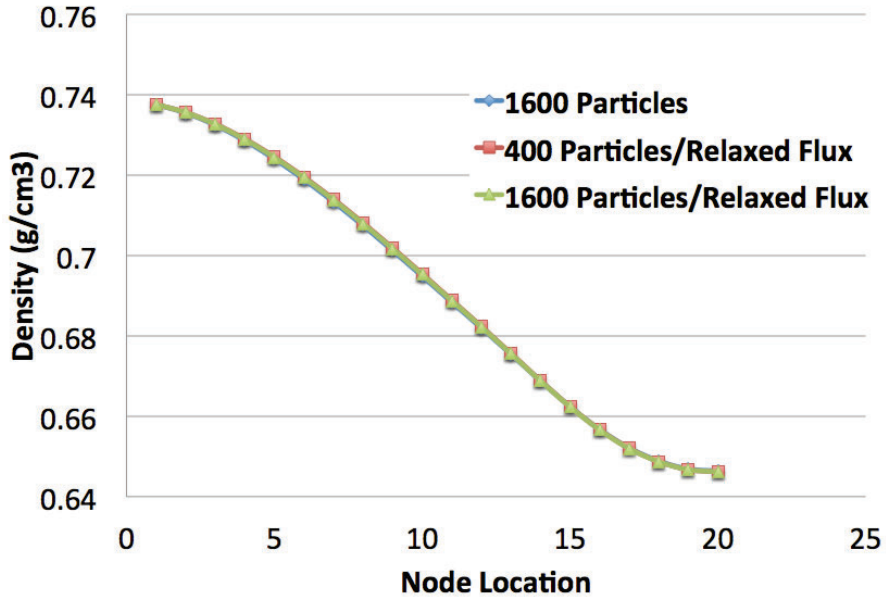


Figure 4 - Average Coolant Density

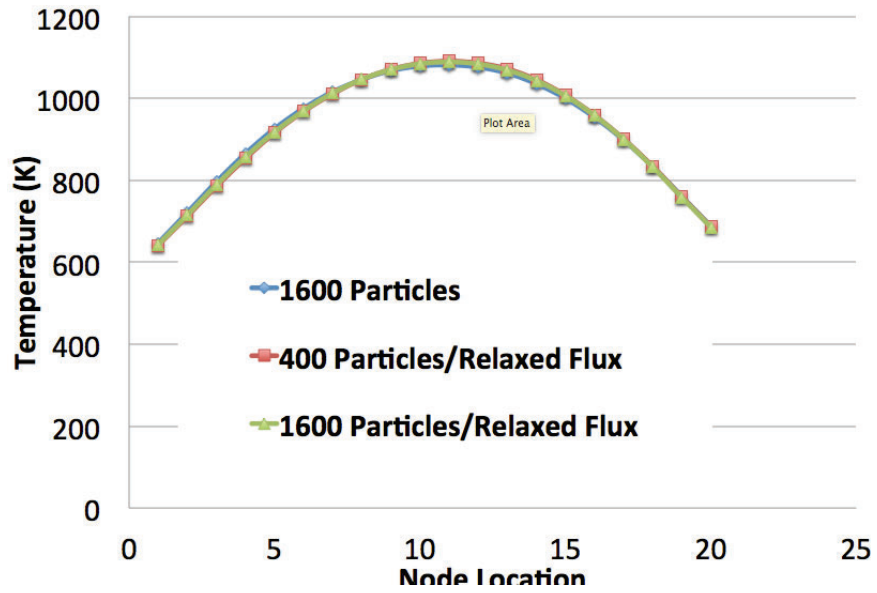


Figure 5 - Average Fuel Temperature

**Table 2 - Average Percent Differences**

	<b>Average % Difference</b>	
<b>Particles/Cycle</b>	<b>400</b>	<b>1600</b>
<b>Fuel Temperature</b>	0.6833	0.5376
<b>Axial Power</b>	2.1254	1.9943
<b>Density</b>	0.0482	0.0360

## **8. Detector Results**

In [7], experimental results were given for some of the assemblies. Their experimental results were obtained by having a detector in each of the instrument tubes while the reactor was at Hot Zero Power (HZP), or about 25 MWth. The detector results were then normalized to have an average of one so that they could be compared with the coupled code results. The detector results come from assembly J10 which has an enrichment of 2.4% and also contains 12 burnable absorber rods. The assembly that was modeled for the coupled calculation has an enrichment of 2.4% but no burnable absorber rods.

The coupled code was run at the following conditions:

- HZP
- 400 Particles/Cycle
- 100 Inactive Cycles
- 400 Active Cycles
- Coupled Convergence =  $1e-4$
- Using Relaxation Acceleration

The coupled calculation was further accelerated by starting with an initial axial power profile of a cosine distribution rather than a uniform distribution. The coupled code calculation converged in 5 iterations. The plot of axial power profile from the coupled calculation and for the detector results is shown in Fig. 6.

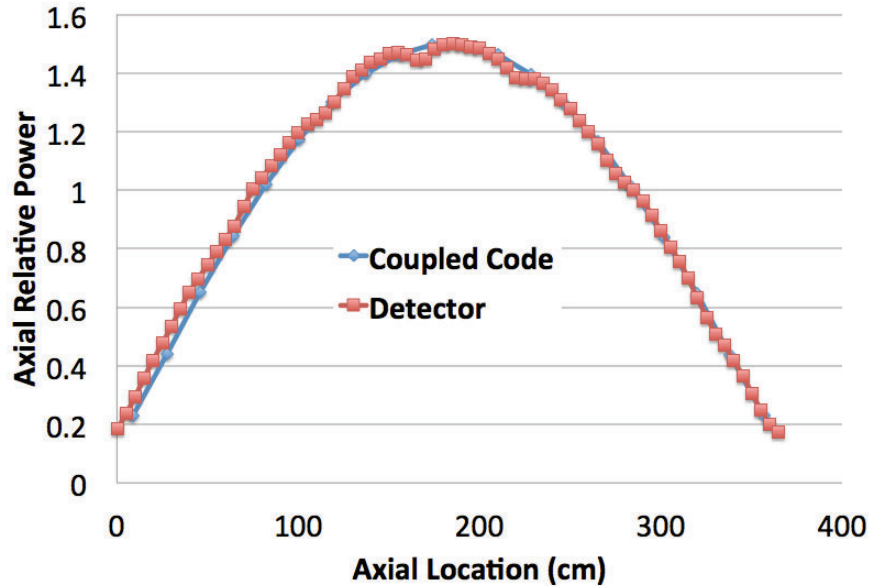


Figure 6 - Axial Power Distribution at HZP

As one can see from Fig. 6, the detector results and the coupled code results show similar results. The main difference in the results is the small drops that are in the detector results. These result from the spacer grids. The spacer grids were not modeled in the coupled calculation.

## 9. Conclusions

This paper presents a coupled MCNP6/CTF code. The coupled code uses On-The-Fly cross sections to decrease the complexity of using a coupled Monte Carlo/thermal-hydraulics code and to decrease the memory requirement. The relaxation acceleration technique was applied to the coupled code. The acceleration technique showed similar results when using the same convergence criteria as the standard approach. In practicality, the convergence criteria will have to be stricter when using this technique but less particles will need to be run. The technique was also able to decrease the statistical error with increasing number of iterations by making the flux a function of all the previous values of the flux estimates during coupled iterations. This also allows a stricter coupled convergence to be obtained than is possible with the standard coupling approach. The comparison of the coupled code predictions with measured data shows a good agreement having in mind that the coupled code did not model all the experimental details.

## REFERENCES

1. A. Bennett, K. Ivanov, and M. Avramova, “Development and Testing of a Coupled MCNP6/CTF Code”, *ANS MC2015*, Nashville, Tennessee.
2. J. T. Goorley, “Initial MCNP6 Release Overview,” *la-ur-13-22934*, Los Alamos National Labs, 2013, [https://laws.lanl.gov/vhosts/mcnp.lanl.gov/pdf\\_files/la-ur-13-22934.pdf](https://laws.lanl.gov/vhosts/mcnp.lanl.gov/pdf_files/la-ur-13-22934.pdf).
3. W. R. Martin, “Implementation of On-The-Fly Doppler Broadening in MCNP,” *la-ur-13-20662*, 2013, [https://laws.lanl.gov/vhosts/mcnp.lanl.gov/pdf\\_files/la-ur-13-20662.pdf](https://laws.lanl.gov/vhosts/mcnp.lanl.gov/pdf_files/la-ur-13-20662.pdf).
4. F. B. Brown, “The makxsf code with Doppler Broadening,” *la-ur-06-7002*, 2006, [https://laws.lanl.gov/vhosts/mcnp.lanl.gov/pdf\\_files/la-ur-06-7002.pdf](https://laws.lanl.gov/vhosts/mcnp.lanl.gov/pdf_files/la-ur-06-7002.pdf).
5. R. Salko and M. Avramova, “CTF Theory Manual,” The Pennsylvania State University, 2014.
6. A. Ivanov, V. Sanchez, R. Stieglitz, K. Ivanov,” Internal multi-scale multi-physics coupled system for high fidelity simulation of light water reactors”, *Annals of Nuclear Energy*, vol. (66C) , pp. 104 – 112, (2014)
7. N. Horelik, B. Herman, B. Forget, K. Smith “Benchmark for Evaluation And Validation of Reactor Simulations(BEAVRS), v1.0.1.”, *Proc. Int. Conf. Mathematics and Computational Methods Applied to Nuc. Sci. & Eng.*, 2013. Sun Valley, Idaho.

## APPENDIX A: Material Specifications

### Fuel: 2.4% Enriched UO<sub>2</sub>

Material	Number Density
U-238	2.2407e-2
U-235	5.5814e-4
U-234	4.4842e-6
O-16	4.5828e-2

### Zircaloy 4

Material	Number Density
Zr-90	2.1827e-2
Zr-91	4.7600e-3
Zr-92	7.2758e-3
Zr-94	7.3734e-3
Zr-96	1.1879e-3
O-16	3.0743e-4
Fe-56	1.3610e-4
Sn-118	1.1669e-4
Sn-120	1.5697e-4

### Borated Water

Material	Number Density
H-1	4.9457e-2
O-16	2.4672e-2
B-10	8.0042e-6
B-11	3.2218e-5